Phosphonated Calixarene as a "Molecular Glue" for Protein Crystallization

Phosphonated Calixarene as a "Molecular Glue" for Protein Crystallization

Jimi M. Alex,[a] Martin L. Rennie,[a] Stefano Volpi,[b] Francesco Sansone,[b] Alessandro Casnati,[b] and Peter B. Crowley*,[a]

[a]School of Chemistry, National University of Ireland Galway, University Road, Galway, Ireland

[b]Dipartimento di Scienze Chimiche, della Vita e della Sostenibilità Ambientale, Università degli Studi di Parma, Viale delle Scienze 17/A, 43124 Parma, Italy

Correspondence: peter.crowley@nuigalway.ie +353 91 49 24 80

KEYWORDS

assembly, cytochrome *c*, lysine recognition, patchy particle, X-ray crystallography

ABSTRACT

Protein crystallization remains a serious bottleneck to structure determination by X-ray diffraction methods. Compounds acting as 'molecular glue' provide a promising strategy to overcome this bottleneck. Such molecules interact *via* non-covalent bonds with two or more protein surfaces to promote lattice formation. Here, we report a 1.5 Å resolution crystal structure of lysine-rich cytochrome *c* complexed with *p*-phosphonatomethyl-calix[4]arene (**pmclx$_4$**). Evidence for complex formation in solution was provided by NMR studies. Similar to *p*-sulfonato-calix[4]arene (**sclx$_4$**), the cavity of **pmclx$_4$** entrapped a single lysine side chain. Interesting features of protein recognition by the phosphonate substituents were identified in the crystal structure. A new calixarene binding site was identified at Lys54. The electron density at this site indicated two distinct calixarene conformers, suggesting a degree of ligand mobility. The role of **pmclx$_4$** in protein crystal packing (molecular glue and patchy particle model) as well as differences in protein-binding with respect to **sclx$_4$** are discussed.

INTRODUCTION

X-ray crystallography is the principal technique for protein structure determination at atomic resolution and the need for diffraction-quality crystals renders protein crystallization a serious bottleneck.[1-3] Protein crystals are finding applications also in catalysis and sensing.[4-6] Considering that the protein is the main variable in crystallization,[7] various methods such as truncation, site-directed mutagenesis and lysine methylation (surface entropy reduction) have been utilized to achieve crystal growth of hard-to-crystallize proteins.[8-12]

An alternative strategy to covalent modification of the protein is the use of additives that prompt assembly and crystallization by interacting with protein surfaces. In view of this approach, a repertoire of compounds have been employed to achieve crystallization of recalcitrant proteins. Examples include dicarboxylic acids / diamino derivatives,[13-15] pyrene-tetrasulfonic acid,[16] polyoxometalates,[17,18] and most recently the crystallophore.[19] We have been tackling the problem by using *p*-sulfonato-calix[4]arene (**sclx$_4$**, Figure 1), a highly water soluble supramolecular building block. Similar to the molecular tweezers,[20,21] this anionic, bowl shaped compound provides a hydrophobic cavity that can accommodate amino acids,[22] in particular, the cationic side chains of lysine and arginine.[23-25] Crystal structures of **sclx$_4$** in complex with the cationic proteins cytochrome *c*[26] and lysozyme,[27,28] suggest that the calixarene acts as a 'molecular glue' to drive protein crystallization.

A great variety of calix[4]arenes have been synthesized with different functional groups at the upper rim to facilitate host-guest supramolecular chemistry.[29,30] Considering the utility of sulfonated-calixarenes for protein binding[22-32] we were motivated to investigate the 'molecular glue' property of other anionic calixarenes. Phosphonate-containing calixarenes[33] have been developed for protein binding[34-36] and recently, we reported the structure and assembly of cytochrome *c* in complex with phosphonato-calix[6]arene (**pclx$_6$**).[37] Here, we demonstrate co-crystallization between *p*-phosphonatomethyl-calix[4]arene[38,39] (**pmclx$_4$**, 800 Da, Figure 1) and cytochrome *c*. In contrast to **sclx$_4$** with the sulfonate anion fixed in the plane of the aromatic ring, the phosphonatomethyl substituent of **pmclx$_4$** can switch between distinct conformations. We were interested to study the impact of this different substituent (and charge distribution) on the protein binding capacity of the ligand.

A 1.5 Å resolution crystal structure provided a detailed view of how **pmclx$_4$** binds to cytochrome *c*. Complex formation was observed at Lys86, which enabled a direct comparison with the structure of a Bromo-functionalized sulfonato-calixarene[31] that also binds this residue. A new binding site was observed at Lys54, though this feature was not evident in NMR solution studies. The molecular recognition capacity and binding affinity imparted by the phosphonatomethyl substituent is discussed. The crystal structure and solution-state studies illustrate the two-sided role of **pmclx$_4$** as a lysine recognition agent and as molecular glue. Furthermore, we suggest that protein surface decoration by calixarenes may provide additional "sticky patches" for crystallization.[12]

EXPERIMENTAL SECTION

Materials. The ligand 5,11,17,23-tetra-(methylphosphonic acid)-25,27,26,28-tetrahydroxycalix[4]arene (**pmclx$_4$**) was (1) used as presented in the protein crystallization additive kit CALIXAR (Molecular Dimensions) or (2) synthesized[38,39] and prepared as a 50 mM solution in water at pH 6.0. Samples of ^{15}N-labelled and unlabelled *Saccharomyces cerevisae* cytochrome *c* C102T were produced by established methods.[26,40]

Protein-ligand co-crystallization. Cytochrome *c* – **pmclx$_4$** co-crystals were grown at 20° C using the hanging drop vapor diffusion method. Hanging drops were prepared with 2 µL of 1.5 mM oxidized cytochrome *c*, 0.4 µL of 3.0 or 5.0 mM **pmclx$_4$** and 1.6 µL of the reservoir. Crystals were obtained at 17-25 % of PEG 3350, 8000 or 10000, in 50 mM NaCl and 50 mM sodium acetate at pH 5.6 (Figure 2). Control drops lacking **pmclx$_4$** remained devoid of crystals.

Data collection. Crystals of ~150 µm dimension (Figure 2D) were cryo-protected in the reservoir solution supplemented with 20 % glycerol and cryo-cooled in liquid nitrogen. Diffraction data were collected at 100° K at beamline 24-ID-C (Advanced Photon Source, Argonne National Laboratory, Argonne, IL) with a Pilatus 6M-F detector. The dataset was collected from a single crystal using ϕ scans of 0.1° over 200°.

Structure determination. The observed reflections were reduced, merged, and scaled with XDS.[41] AIMLESS[42] revealed anisotropic diffraction extending to 1.2 Å along 0.57 h + 0.82 l and k axes and 1.5 Å along -0.47 h + 0.88 l axis as indicated by $CC_{1/2}$ (> 0.3). Data extending to 1.5 Å was used for model building and refinement. The structure was determined by molecular replacement in PHASER[43] with PDB 1YCC as the search model. The coordinates for **pmclx$_4$** were built in JLigand[44] and added to the model in COOT.[45] Iterative cycles of manual model building and refinement (in REFMAC5 as implemented in CCP4[46]) was continued until no further improvements in R_{free} or electron density were obtained. The structure was validated with MolProbity[47] and deposited in the Protein Data Bank (PDB 5NCV).

Accessible surface area (ASA) calculations. The effect of **pmclx$_4$** on the ASA of cytochrome *c* residues in the crystal structure was determined in AreaIMol,[46] according to equations 1 and 2. These calculations take into account the ASA of residues in the crystal packing environment in the absence (A_{pro}, Å^2) and presence ($A_{pro+lig}$, Å^2) of the ligand. We define Y_{lig} (Å^2), the ASA of each residue in the presence of ligand in the crystal packing environment and X_{free} (Å^2), the ASA of residues in the free protein (ignoring ligand and crystal packing). Z_{lig} (Å^2) is the area that remains accessible.

$$Y_{lig} = A_{pro} - A_{pro+lig} \quad \textbf{(1)}$$

$$Z_{lig} = X_{free} - Y_{lig} \quad \textbf{(2)}$$

In Figure 6, X_{free} and Z_{lig} are plotted as black and grey bars, respectively.

NMR spectroscopy. The typical sample composition was 0.1 mM ^{15}N cytochrome *c* in 20 mM KH_2PO_4, 50 mM NaCl, 1 mM sodium ascorbate, 10 % D_2O at pH 6.0. NMR titrations were performed at 303 K using 0.5-32 µL aliquots of a 50 mM **pmclx$_4$** stock. ^{1}H-^{15}N HSQC spectra were acquired with spectral widths of 16 ppm (^{1}H) and 40 ppm (^{15}N) on a 600 MHz Varian spectrometer equipped with a HCN coldprobe.[26] Analysis of the ligand-induced chemical shift perturbations was performed in CCPNmr.[48]

NMR-derived binding curves. Binding isotherms were obtained by plotting the chemical shift changes (Δδ) as a function of the ligand concentration. The data were fit globally in Origin by using a 1:1 binding model (Equation 3).

$$\Delta\delta = \Delta\delta_{max} \frac{[A_T]+[B_T]+[K_d]-\sqrt{([A_T]+[B_T]+[K_d])^2-4[A_T][B_T]}}{2[B_T]} \quad \textbf{(3)}$$

Where, $[A_T]$ and $[B_T]$ were the ligand and protein concentrations, respectively.

RESULTS AND DISCUSSION

Cytochrome *c* – pmclx$_4$ co-crystallization. pmclx$_4$ was identified initially as a ligand for cytochrome *c* crystallization by using the CALIXAR Kit (Molecular Dimensions). Co-crystals of **pmclx$_4$** and cytochrome *c* were obtained from conditions similar to those reported for **sclx$_4$**.[26] While 10 equivalents of **sclx$_4$** were required to achieve crystal growth, <1 equivalent of ligand were sufficient to obtain cytochrome *c* – **pmclx$_4$** co-crystals. Crystals grew reproducibly in a range of PEG molecular weights and concentrations (17-25 % PEG 3350, 8000 or 10000) in 50 mM NaCl and 50 mM sodium acetate pH 5.6 (Figure 2). In the absence of **pmclx$_4$** there was no crystal growth, indicating that the ligand was necessary for crystallization under these conditions.

X-ray structure of cytochrome *c* – pmclx$_4$. A single crystal (Figure 2D) resulted in anisotropic diffraction (1.2 Å resolution in two directions and 1.5 Å in the third direction). Structure determination in PHASER[41] yielded two protein molecules (chains A and B), and three calixarenes in the asymmetric unit (Figure 3A). There was no electron density for the four N-terminal residues (including Lys-2) in either protein chain, indicative of disorder. The presence of two cytochrome *c* molecules in the asymmetric unit was similar to other calixarene-bound structures.[26,31,37] All three calixarenes were modeled at sites where they encapsulated a single lysine residue, Lys86 in chains A and B and Lys54 in chain A only.

In the protein-bound form, the phosphonate substituents of **pmclx$_4$** occurred in two distinct conformations. Either all four substituents were splayed outwards (away from the cavity) or one was turned inwards (toward the cavity). While both conformations permitted complete encapsulation of one lysine side chain they resulted in markedly different protein-calixarene interactions (Figure 3B). For example, at Lys86 in chain A (A.Lys86) there was no salt bridge interaction between the lysine ammonium group and the phosphonates. Instead, the ammonium group was solvated by 3 water molecules. In contrast, at Lys86 in Chain B (B.Lys86) one of the phosphonatomethyl groups was rotated into the cavity permitting salt bridge formation to the lysine. In this case, the ammonium was solvated by one water molecule.

Similar features occurred at Lys54 in chain A (A.Lys54) site. Here, it was necessary to model two calixarenes (70:30 occupancy) to account for the electron density (Figure 4B and

Figure S1). The two models differed most by a rotation of one phosphonatomethyl group and the higher occupancy conformer had a salt bridge to the lysine ammonium ($N^{\zeta}\cdots$O-P = 3.1 Å). This phosphonate also hydrogen bonded with the backbone carbonyl of Lys54 (CO$\cdots$O-P = 2.8 Å). The requirement for two conformations at this site suggested that ligand binding was less well defined. Interestingly, this site was not detected in NMR experiments (*vide infra*). Lys54 is flanked by hydrophobic side chains, Ala51 and Ile53, both of which were in van der Waals contact with an upper rim $-CH_2-$ of **pmclx$_4$**. Polar side chains contributed also with hydrogen bonds from Asp50 and Asn56 to the phosphonates.

Lysine encapsulation by **pmclx$_4$** had some similarities with **sclx$_4$** including cation-π and CH-π bonds with the Lys-C^{ε}.[26] However, the complexes formed by these ligands differed crucially in the degree of salt bridge formation with the lysine ammonium group. In **pmclx$_4$** a single phosphonate alternated in/out (Figures 3B and 4B), while in **sclx$_4$** (with the anion fixed in the plane of the aromatic ring) salt bridges were formed with one or two sulfonates. The sulfonate also had a tendency to hydrogen bond with backbone amide NHs. No such interactions were observed with **pmclx$_4$**. Similarities with the bromine-functionalized sulfonato-calixarene **Br.sclx**, should be noted, as this ligand bound also to Lys86 (Figure 5).[31]

Crystal Packing Interactions. Applying the symmetry operations to the asymmetric unit revealed a close-packed structure (Figure 4A) and nine cytochrome *c*–**pmclx$_4$** interfaces, ranging in size from 30-300 Å^2 (Table 1). Interestingly, the A.Lys54 and B.Lys86 complexes were positioned adjacent to each other and sandwiched Lys4 (Figure 4B). Together the two ligands masked ~90 % of this Lys4 (Figure 6) *via* multiple interactions including salt bridges ($N^{\zeta}\cdots$O-P ~3.0 Å), and CH-π / cation-π bonds (Lys4-C^{ε}/$C^{\delta}\cdots$centroid ~4.0 Å).

Crystal packing also involved direct or water-mediated salt bridges, for example, A.Lys54 **pmclx$_4$** with Lys5, Lys22, Lys73 and Lys89. And B.Lys86 **pmclx$_4$** formed a cation-π bond to Lys100 and an edge-to-face π$\cdots$π interaction with Tyr97 ($C^{\varepsilon}\cdots$centroid = 3.8 Å). The C^{β} atoms of Ala7 and Ala101 (which flank Tyr97) were in van der Waals contact with methylene bridges of **pmclx$_4$**. Interestingly, this hydrophobic binding patch was identified previously in the complexes with a phenyl-substituted sulfonato-calixarene (**Ph.sclx**)[31] and with **pclx$_6$**.[37] Two other interactions merit

mention here. It has been observed previously that the calixarene lower rim phenolic hydroxyls make van der Waals' contact with the C^{β} of alanine.[26,31] This same feature was evident at B.Lys86 **pmclx$_4$**. At A.Lys54 **pmclx$_4$** the phenolic hydroxyls were hydrogen bonded to a water molecule and to the hydroxyl of Thr8.

The varying contributions of all lysines to ligand binding were evident from ASA calculations (methods and Figure 6). Of the most accessible residues; Lys4, Lys11, Lys54, Lys73 and Lys86 (ASA > 150 Å^2), **pmclx$_4$** selected Lys86. On the other hand Lys55, Lys79 and Lys99 were least accessible (ASA < 100 Å^2) and did not contribute to ligand binding. The substantially different contributions from each protein chain are also evident, as discussed for Lys54. Similarly, Lys5 from chain A was largely involved in ligand binding, while in chain B it did not interact with **pmclx$_4$**.

Lysine encapsulation by **pmclx$_4$** resulted in ~300 Å^2 of protein surface coverage (Table 1, similar to **sclx$_4$**[26]). In addition to masking this surface area, the calixarene contributed a new surface of ~600 Å^2 to the particle. This patch size is equivalent to a protein crystal packing interface[49] and, as discussed, provides a surface that can participate in numerous noncovalent interactions with adjacent proteins in the crystal (Figure 4B) consistent with a "molecular glue" functionality.[26,31,37] Notably, the exposed surface of the calixarene is equivalent to ~10 % of the cytochrome *c* surface area. Therefore, it appears that protein surface decoration by calixarenes may be a special case of the patchy particle model of protein crystallization.[12,50,51]

NMR Characterization and Comparison with the Solid State. Protein-ligand titrations were performed by the addition of microliter aliquots of 50 mM **pmclx$_4$** to ^{15}N-labelled cytochrome *c*, which was monitored by ^{1}H-^{15}N HSQC. The overlaid HSQC spectra (Figure 7) revealed increasing chemical shift perturbations (Δδ) as a function of the **pmclx$_4$** concentration, indicative of fast-intermediate exchange between the ligand-free and -bound states. However, the resonances of Leu85 and Lys87 exhibited strongly biphasic chemical shift perturbations and some resonances were broadened beyond detection at ~4 (Lys4) or ~6 eq. (Lys11 and Leu85) of **pmclx$_4$**. Spectral broadening might indicate intermediate exchange or multiple conformations adopted by these residues. Significant perturbations ($^1H^N \geq 0.04$ ppm or $^{15}N \geq 0.4$ ppm) were observed for 37

resonances, including Lys-2, Lys4, Lys5, Lys73, Lys86, Lys87, Lys89 and Lys100. These residues (except Lys-2), participated in multiple non-covalent interactions at protein-calixarene interfaces in the crystal structure (Figures 4B and 5). While the large NMR effects for Leu85, Lys86 and Lys87 are consistent with the crystal structure (complex formation at Lys86, Figure 3B) there were also some contrasting results. For example, Lys11 did not contribute to complex formation in the crystal structure (Figure 5) yet this resonance was broadened beyond detection. Conversely, Lys54 did not exhibit a significant Δδ yet complex formation was observed at this residue in the crystal (*vide supra*, Figure 3). A similar observation was made in the cytochrome *c* – **sclx$_4$** complex in which Lys22, a binding site observed in the crystal structure, was not affected in the NMR.[26] Overall, these results suggest that complex formation occurred with slight differences in the solution and solid states. While binding to Lys54 may be the result of the crystallization conditions/environment other differences may be attributed to the fluxionality of calixarene binding, which likely involves ligand hopping between lysine side chains.[26,31]

Apparent dissociation constants were calculated from titration data collected up to ~6 eq. of **pmclx$_4$**. The binding isotherms (Figure 7B) were hyperbolic and fit to a 1:1 binding model (Equation 3). The average *apparent* K_d of 0.04 (± 0.01) mM was at least 10-fold stronger than for the complex with **sclx$_4$**.[26] The tighter binding of **pmclx$_4$** agrees with the observation that protein crystallization occurred at approximately ten-fold lower equivalents of this ligand compared to **sclx$_4$**. Features such as the increased hydrogen-bonding capacity of phosphonate versus sulfonate, the mobility of the anionic substituent, as well as the increased hydrophobicity of the cavity (upper rim –CH_2– substituents) likely contribute to the tighter binding of **pmclx$_4$**.

CONCLUSIONS

The cytochrome *c* – **pmclx$_4$** crystal structure illustrates the utility of the phosphonatomethyl substituent as a contributor to stronger, higher specificity 'molecular glue' properties compared to the sulfonate.[26] Cytochrome *c* – **pmclx$_4$** crystal growth was achieved with ~10-fold less ligand than was required to obtain cytochrome *c* – **sclx$_4$** co-crystals. While **sclx$_4$** occupied three different sites (Lys4, Lys22 and Lys89) on the protein surface, **pmclx$_4$** bound to two different sites (Lys54 and Lys86) suggesting increased specificity of **pmclx$_4$** in the solid state.

Interestingly, lysine encapsulation occurred with the presence or absence of a salt bridge to one phosphonatomethyl substituent that could rotate into the cavity. In contrast, the sulfonate substituents always formed one or more salt bridges to the lysine. The phosphonatomethyl functionalized calixarenes may prove beneficial for achieving crystal growth of cationic proteins, in particular nucleic acid binding proteins. More generally, protein surface decoration by calixarenes may provide the necessary "sticky patches" that facilitate packing contacts and crystal growth.[12,50,51]

ASSOCIATED CONTENT

Supporting Information

Figure S1. A.Lys54 binding site

Table S1. X-ray data collection, processing and refinement statistics for cytochrome c - **pmclx$_4$**

AUTHOR INFORMATION

Corresponding Author

peter.crowley@nuigalway.ie +353 91 49 24 80

Author Contributions

JMA and PBC designed the experiments. SV, FS and AC synthesised the calixarene. JMA performed the crystallization experiments and NMR data collection. MLR collected the synchrotron data and helped to solve the structure. JMA and PBC analyzed the data and wrote the paper. All of the authors contributed to the final version of the manuscript.

Funding Sources

This research was supported by NUI Galway (Hardiman Research Scholarship to JMA), Science Foundation Ireland (grants 13/ERC/B2912 and 13/CDA/2168 to PBC) and Università di Parma (FIL project).

ACKNOWLEDGMENT

We thank A. R. Khan (TCD), APS synchrotron for beam time allocation, and the staff at beamline 24-ID-C for assistance with data collection. A. M. Doolan is acknowledged for technical support. We thank also Centro Interdipartimentale di Misure (Parma) for mass and NMR facilities.

REFERENCES

1. Garman, E. F. *Science* **2014**, *343*, 1102-1108.
2. Sauter, A.; Roosen-Runge, F.; Zhang, F.; Lotze, G.; Jacobs, R. M. J.; Schreiber, F. *J. Am. Chem. Soc.* **2015**, 137, 1485-1491.
3. Schubert, R.; Meyer, A.; Baitan, D.; Dierks, K.; Perbandt, M.; Betzel, C. *Cryst. Growth Des.* **2017**, 17, 954-958.
4. McGovern, R. E.; Feifel, S.C.; Lisdat, F.; Crowley, P. B. *Angew. Chem. Int. Ed.* **2015**, *54*, 6356-6359.
5. Abe, S.; Maity, B.; Ueno, T. *Curr. Opin. Chem. Biol.* **2017**, *43*, 68-76.
6. Lopez, S.; Rondot, L.; Leprêtre, C.; Marchi-Delapierre, C.; Ménage, S.; Cavazza, C. *J. Am. Chem. Soc.* **2017**, *139*, 17994-18002.
7. Longenecker, K. L.; Garrard, S. M.; Sheffield, P. J.; Derewenda, Z. S. *Acta Crystallogr. D* **2001**, *57*, 679-688.
8. Walter, T. S.; Meier, C.; Assenberg, R.; Au, K. F.; Ren, J.; Verma, A.; Nettleship, J. E.; Owens, R. J.; Stuart, D. I.; Grimes, J. M. *Structure* **2006**, *14*, 1617-1622.
9. Cooper, D. R.; Boczek, T.; Grelewska, K.; Pinkowska, M.; Sikorska, M.; Zawadzki, M.; Derewenda, Z. *Acta Crystallogr. D* **2007**, *63*, 636-645.
10. Price II, W. N.; Chen, Y.; Handelman, S. K.; Neely, H.; Manor, P.; Karlin, R.; Nair, R.; Liu, J.; Baran, M.; Everett, J.; Tong, S. N.; Forouhar, F.; Swaminathan, S. S.; Acton, T.; Xiao, R.; Luft, J. R.; Lauricella, A.; DeTitta, G. T.; Rost, B.; Montelione, G. T.; Hunt, J. F. *Nat. Biotech.* **2009**, *27*, 51-57.
11. Sledz, P.; Zheng, H.; Murzyn, K.; Chruszcz, M.; Zimmerman, M. D.; Chordia, M. D.; Joachimiak, A.; Minor, W. *Protein Sci*. **2010**, *19*, 1395-1404.
12. Derewenda, Z. S.; Godzik, A. *Methods Mol. Biol.* **2017**, *1607*, 77-115.
13. McPherson, A.; Cudney, B. *J. Struct. Biol.* **2006**, *156*, 387-406.
14. Larson, S. B.; Day, J. S.; Cudney, R.; McPherson, A. *Acta Crystallogr. D* **2007**, *63*, 310-318.
15. McPherson, A.; Nguyen, C.; Cudney, R.; Larson, S. B. *Cryst. Growth Des.* **2011**, *11*, 1469-1474.
16. Morgan, H. P.; McNae, I. W.; Hsin, K.-Y.; Michels, P. A.; Fothergill-Gilmore, L. A.; Walkinshaw, M. D. *Acta Crystallogr. F* **2010**, *66*, 215-218.

17. Bijelic, A.; Rompel, A. *Acc. Chem. Res.* **2017**, *50*, 1441-1448.
18. Zebisch, M.; Krauss, M.; Schäfer, P.; Straeter, N. *Acta Crystallogr. D* **2014**, *70*, 1147-1154.
19. Engilberge, S.; Riobé, F.; Di Pietro, S.; Lassalle, L.; Coquelle, N.; Arnaud, C.-A.; Pitrat, D.; Mulatier, J.-C.; Madern, D.; Breyton, C.; Maury, O.; Girard, E. *Chem. Sci.* **2017**, *8*, 5909-5917.
20. Bier, D.; Rose, R.; Bravo-Rodriguez, K.; Bartel, M.; Ramirez-Anguita, J. M.; Dutt, S.; Wilch, C.; Klärner, F.-G.; Sanchez-Garcia, E.; Schrader, T.; Ottmann C. *Nat. Chem.* **2013**, *5*, 234-239.
21. Trusch, F.; Kowski, K.; Bravo-Rodriguez, K.; Beuck, C.; Sowislok, A.; Wettig, B.; Matena, A.; Sanchez-Garcia, E.; Meyer, H.; Schrader, T.; Bayer, P. *Chem. Commun.* **2016**, *52*, 14141-14144.
22. Atwood, J. L.; Ness, T.; Nichols, P. J.; Raston, C. L. *Cryst. Growth Des.* **2002**, *2*, 171-176.
23. Selkti, M.; Coleman, A. W.; Nicolis, I.; Douteau-Guével, N.; Villain, F.; Tomas, A.; de Rango, C. *Chem. Commun.* **2000**, 161-162.
24. Lazar, A.; Da Silva, E.; Navaza, A.; Barbey, C.; Coleman, A. W. *Chem. Commun.* **2004**, *19*, 2162-2163.
25. Beshara, C. S.; Jones, C. E.; Daze, K. D.; Lilgert, B. J.; Hof, F. *ChemBioChem.* **2010**, *11*, 63-66.
26. McGovern, R. E.; Fernandes, H.; Khan, A. R.; Power, N. P.; Crowley, P. B. *Nat. Chem.* **2012**, *4*, 527-533.
27. McGovern, R. E.; McCarthy, A. A.; Crowley, P. B. *Chem. Commun.* **2014**, *50*, 10412-10415.
28. McGovern, R. E.; Snarr, B. D.; Lyons, J. A.; McFarlane, J.; Whiting, A. L.; Paci, I.; Hof, F.; Crowley, P. B. *Chem. Sci.* **2015**, *6*, 442-449.
29. Giuliani, M.; Morbioli, I.; Sansone, F.; Casnati, A. *Chem. Commun.* **2015**, *51*, 14140-14159.
30. Atwood, J. L. *Comprehensive Supramolecular Chemistry II*, 2nd Edition, **2017**, Elsevier.
31. Doolan, A. M.; Rennie, M. L.; Crowley, P. B. *Chem. Eur. J.* **2018**, *24*, 984-991.
32. Mallon, M.; Dutt, S.; Schrader, T.; Crowley, P. B. *ChemBioChem* **2016**, *17*, 774-783.
33. Martin, A. D.; Raston, C. L. *Chem. Commun.* **2011**, *47*, 9764-9772.
34. Zadmard, R.; Schrader, T. *J. Am. Chem. Soc.* **2005**, *127*, 904-915.
35. Kolusheva, S.; Zadmard, R.; Schrader, T.; Jelinek, R. *J. Am. Chem. Soc.* **2006**, *128*, 13592-13598.
36. Trush, V. V.; Kharchenko, S. G.; Tanchuk, V. Y.; Kalchenko, V.I.; Vovk, A. I. *Org. Biomol. Chem.* **2015**, *13*, 8803-8806

37. Rennie, M. L.; Doolan, A. M.; Raston, C. L.; Crowley, P. B. *Angew. Chem. Int. Ed.* **2017**, *56*, 5517-5521.
38. Almi, M.; Arduini, A.; Casnati, A.; Pochini, A.; Ungaro, R. *Tetrahedron*, **1989**, *45*, 2177-2182. **pmclx$_4$** was obtained after salification with 4 equiv. of 0.1 M NaOH and crystallized as a beige solid upon addition of ethanol.
39. Mourer, M.; Psychogios, N.; Laumond, G.; Aubertin, A.-M.; Regnouf-de-Vains, J.-B. *Bioorg. Med. Chem.* **2010**, *18*, 36-45.
40. Crowley P. B.; Ganji, P; Ibrahim, H. *ChemBioChem* **2008**, *9*, 1029-1033.
41. Kabsch, W. *Acta Crystallogr. D* **2010**, *66*, 125-132.
42. Evans, P. R.; Murshudov, G. N. *Acta Crystallogr. D* **2013**, *69*, 1204-1214.
43. McCoy, A. J.; Grosse-Kunstleve, R. W.; Adams, P. D.; Winn, M. D.; Storoni, L. C.; Read, R. J. *J. Appl. Crystallogr.* **2007**, *40*, 658-674.
44. Potterton, E.; Briggs, P.; Turkenburg, M.; Dodson, E. *Acta Crystallogr. D* **2003**, *59*, 1131-1137.
45. Emsley, P.; Lohkamp, B.; Scott, W. G.; Cowtan, K. *Acta Crystallogr. D* **2010**, *66*, 486-501.
46. Vagin, A. A.; Steiner, R. A.; Lebedev, A. A.; Potterton, L.; McNicholas, S.; Long, F.; Murshudov, G. N. *Acta Crystallogr. D* **2004**, *60*, 2184-2195.
47. Chen, V. B.; Arendall, W. B.; Headd, J. J.; Keedy, D. A.; Immormino, R. M.; Kapral, G. J.; Murray, L. W.; Richardson, J. S.; Richardson, D. C. *Acta Crystallogr. D* **2010**, *66,* 12-21.
48. Vranken, W. F.; Boucher, W.; Stevens, T. J.; Fogh, R. H.; Pajon, A.; Llinas, M.; Ulrich, E. L.; Markley, J. L.; Ionides, J.; Laue, E. D. *Proteins* **2005**, *59*, 687-696.
49. Janin, J.; Bahadur, R. P.; Chakrabarti, P. *Q. Rev. Biophys.* **2008**, *41*, 133-180
50. Fusco, D.; Headd, J. J.; De Simone, A.; Wang, J.; Charbonneau, P. *Soft Matter.* **2014**, *10*, 290-302.
51. Staneva, I.; Frenkel, D. *J. Chem. Phys.* 2015, *143*, 194511-194516.

Tables

Table 1. Interface analysis of the cytochrome *c* – **pmclx$_4$** binding sites.

Protein Site[a]	pmclx$_4$	Interface Area (Å^2)	Total Area (Å^2)
A.Lys54	1	270	540
A1		210	
B		30	
B1		30	
A.Lys86	2	260	550
B2		290	
B.Lys86	3	300	630
A2		265	
B3		65	

[a]*P*12$_1$1 symmetry operations used to generate symmetry mates: **A1**, -x, y-1/2, -z+1; **B1**, x-1, y, z; **B2,** -x, y-1/2, -z+1; **A2**, -x-1, y-1/2, -z; **B3**, x-1, y, z.

Figures

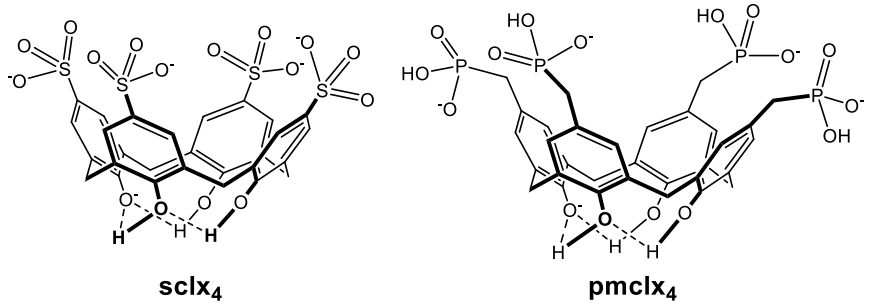

Figure 1. Molecular structures of *p*–sulfonato-calix[4]arene (**sclx$_4$**) and *p* phosphonatomethyl-calix[4]arene (**pmclx$_4$**). Calix[4]arenes adopt a cone conformation due to hydrogen bonding between the phenolic hydroxyls, one of which is deprotonated.

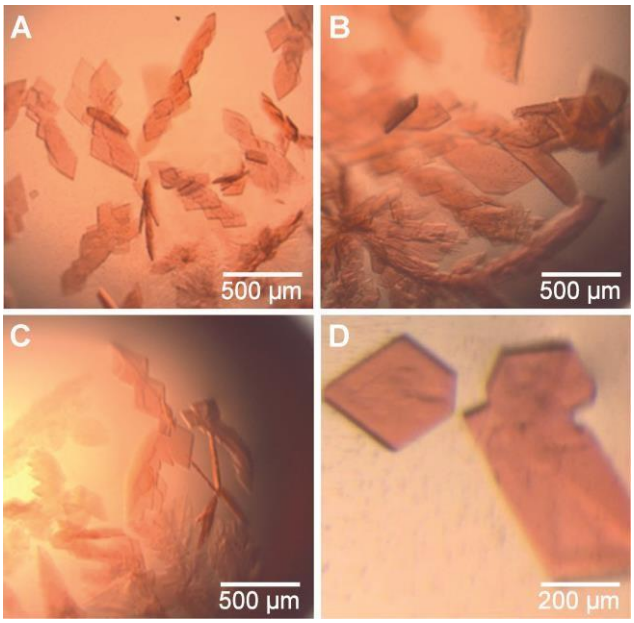

Figure 2. Co-crystals of cytochrome *c* and **pmclx$_4$** grown in hanging drops that contained 17 % **(A)** PEG 3350, **(B)** PEG 8000, **(C)** PEG 10000 or **(D)** 20 % PEG 8000 in 50 mM NaCl and 50 mM sodium acetate pH 5.6. Crystals were obtained at 0.75 mM protein and 0.3 or 0.5 mM ligand. A crystal from **(D)** diffracted to 1.5 Å.

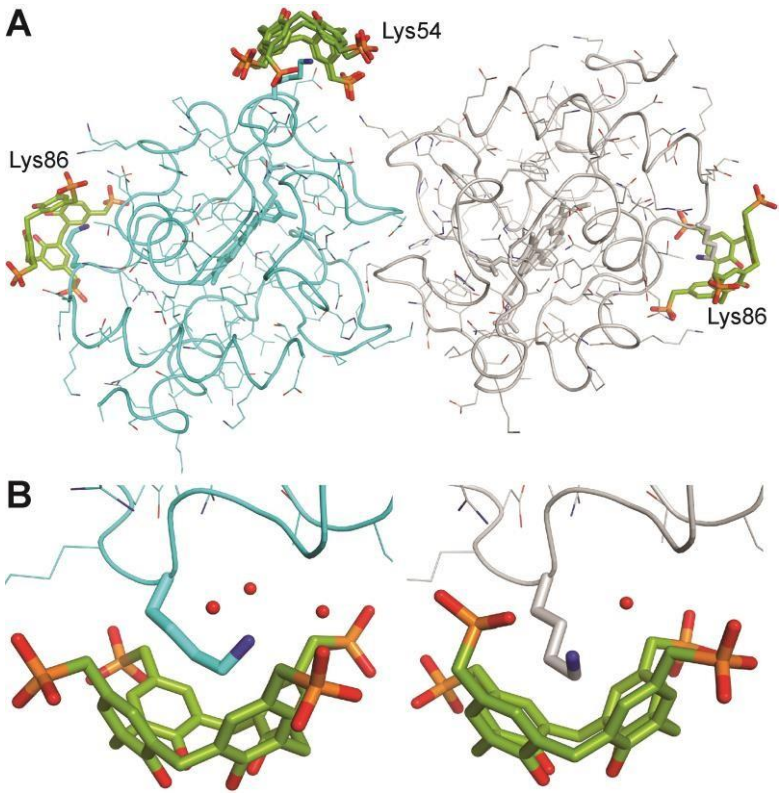

Figure 3. (A) The asymmetric unit of the cytochrome *c* – **pmclx$_4$** complex comprised two molecules of cytochrome *c* (chains A and B in blue and grey), and three molecules of **pmclx$_4$** (PDB 5NCV). The proteins are shown as ribbons with side chains as lines and the entrapped lysines as sticks. **(B)** The Lys86 binding site in chains A and B differ by the absence or presence of a salt bridge to one phosphonate substituent. Note the altered lysine conformation and hydration, with waters indicated as red spheres.

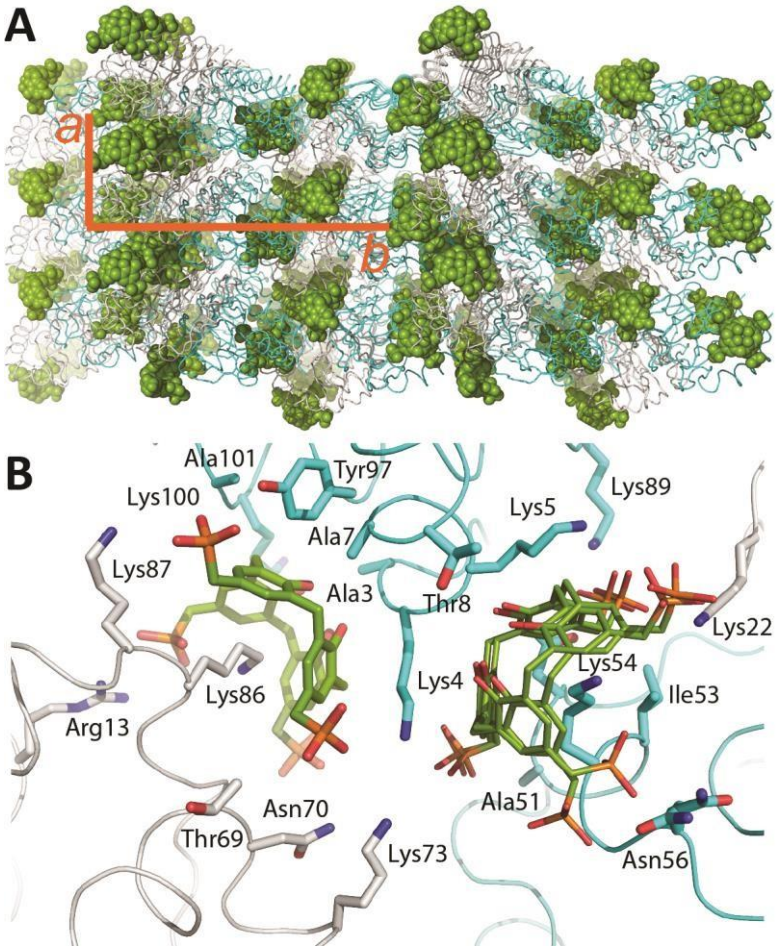

Figure 4. (A) Crystal packing in the cytochrome *c* – **pmclx$_4$** complex. Proteins and ligands are rendered as ribbons and spheres, respectively. The unit cell axes *a*, *b* are indicated. **(B)** 'Molecular glue' contacts between two molecules of pmclx$_4$ and four protein chains (color scheme as per Figure 3). Alternate conformations of the ligand at Lys54 (shown as light sticks) were apparent in the electron density (Figure S1). All side chains within van der Waals contact of the ligands are shown as sticks. Lys4 is sandwiched between two pmclx$_4$ ligands at A.Lys54 and B.Lys86. In addition to Lys-phosphonate salt bridges, numerous other features (labeled side chains) contributed to binding.

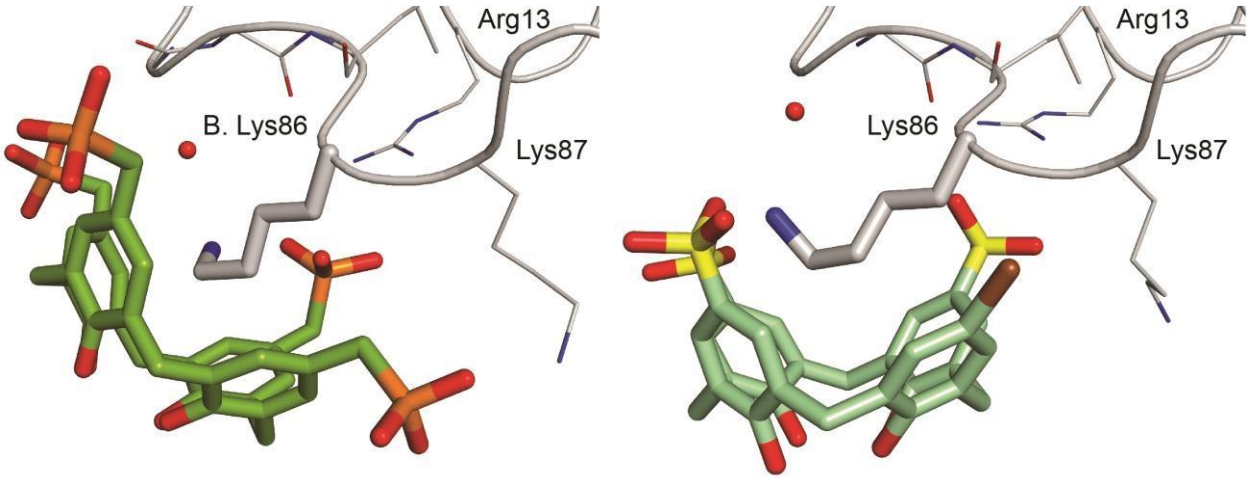

Figure 5. The Lys86 binding site of cytochrome *c* in complex with **pmclx$_4$** or **Br.sclx** (PDB 5LFT[31]). The proteins are oriented identically to highlight differences in the calixarene-protein contacts.

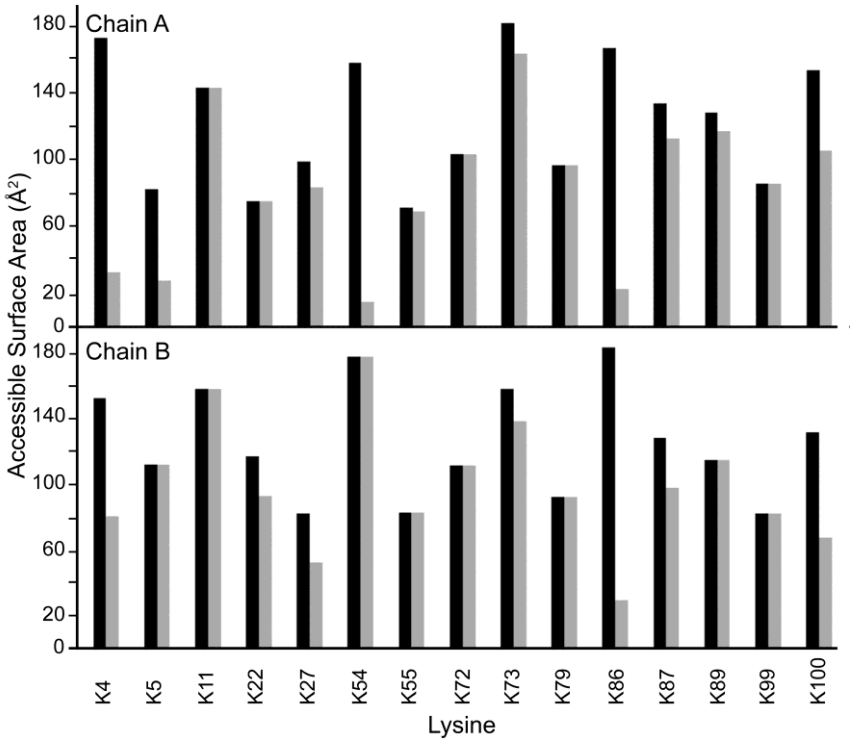

Figure 6. Accessible surface area (ASA) of lysines in the ligand-free (black bars) and -bound (grey) states of cytochrome *c*. The varying contributions of different lysines to **pmclx$_4$** binding in chains A and B are evident. Lys-2 is not shown as this residue was disordered in the crystal structure.

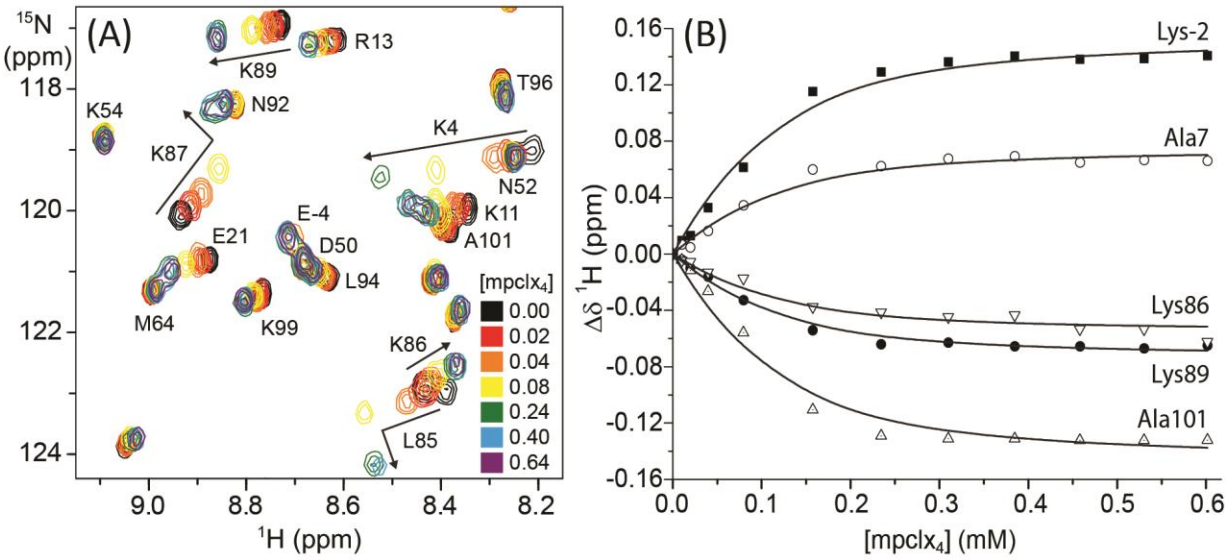

Figure 7. NMR characterization of **pmclx$_4$** binding to cytochrome *c*. **(A)** Region from overlaid ^{1}H-^{15}N HSQC spectra of 0.1 mM pure cytochrome *c* (black contours) and in the presence of 0.02–0.64 mM **pmclx$_4$** (colored scale). Notes: negligible change to Lys54; biphasic shifts for Leu85 and Lys87; and Lys4, Lys11 and Leu85 broadened beyond detection. **(B)** Binding curves for individual resonances were fit globally to a 1:1 binding model to yield K_d ~0.04 mM.

TOC Graphic

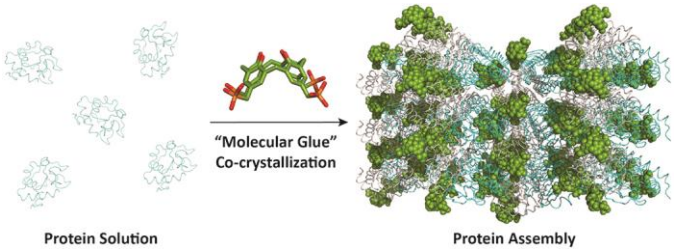

SYNOPSIS

A crystal structure of the cytochrome *c* – **pmclx$_4$** complex highlights the use of anionic calixarenes as 'molecular glue' for protein assembly and crystallization.